BIOCHEMISTRY
including biophysical chemistry & molecular biology

Article

pubs.acs.org/biochemistry

Effect of Charged Amino Acid Side Chain Length on Lateral Cross-Strand Interactions between Carboxylate-Containing Residues and Lysine Analogues in a β-Hairpin

Hsiou-Ting Kuo,[†] Chun-Jen Fang,[†] Hsin-Yun Tsai,[†] Min-Fan Yang,[†] Hsien-Chen Chang,[†] Shing-Lung Liu,[†] Li-Hung Kuo,[†] Wei-Ren Wang,[†] Po-An Yang,[†] Shing-Jong Huang,[‡] Shou-Ling Huang,[‡] and Richard P. Cheng*,[†]

[†]Department of Chemistry, National Taiwan University, Taipei 10617, Taiwan

[‡]Instrument Center at National Taiwan University, National Taiwan University, Taipei 10617, Taiwan

Supporting Information

ABSTRACT: β-Sheets are one of the fundamental three-dimensional building blocks for protein structures. Oppositely charged amino acids are frequently observed directly across one another in antiparallel sheet structures, suggesting the importance of cross-strand ion pairing interactions. Despite the apparent electrostatic nature of ion pairing interactions, the charged amino acids Asp, Glu, Arg, Lys have different numbers of hydrophobic methylenes linking the charged functionality to the backbone. Accordingly, the effect of charged amino acid side chain length on cross-strand ion pairing interactions at lateral non-hydrogen bonded positions was investigated in a β-hairpin motif. The negatively charged residues with a carboxylate (Asp, Glu, Aad in increasing length) were incorporated at position 4, and the positively charged residues with an ammonium (Dap, Dab, Orn, Lys in increasing length) were incorporated at position 9. The fraction folded population and folding free energy were derived from the chemical shift deviation data. Double mutant cycle analysis was used to determine the interaction energy for the potential lateral ion pairs. Only the Asp/Glu-Dap interactions with shorter side chains and the Aad-Orn/Lys interactions with longer side chains exhibited stabilizing energetics, mostly relying on electrostatics and hydrophobics, respectively. This suggested the need for length matching of the interacting residues to stabilize the β-hairpin motif. A survey of a nonredundant protein structure database revealed that the statistical sheet pair propensity followed the trend Asp-Lys < Glu-Lys, also implying the need for length matching of the oppositely charged residues.

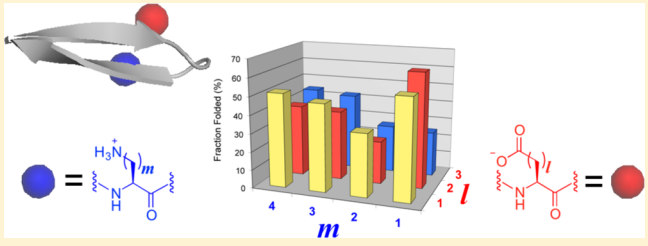

Proteins are biological macromolecules that participate in many vital processes in the cells of living organisms by performing various biochemical functions. The hierarchical nature of protein structure highlights the importance of secondary structures,[1,2] including α-helices and β-sheets, as the fundamental three-dimensional building blocks for proteins. Statistical analysis showed that 36% of the protein residues adopt an α-helix conformation,[3−7] and 23% of the protein residues adopt a β-sheet conformation.[3,8,9] Furthermore, β-sheets are formed during amyloid fibril formation, which plays a major role in various diseases including Alzheimer's disease,[10,11] Huntington's disease,[12,13] Parkinson's disease,[14,15] type II diabetes,[16,17] and Creutzfeldt−Jakob prion disease.[18,19] Misfolded protein conformations, which form β-sheets, are closely associated with these diseases. As such, fundamental studies on model β-sheet structures may provide insight into understanding the molecular basis for sheet formation, stability, and self-association and should contribute to the overall biomedical knowledge of ailments involving undesirable sheet structures.

Statistical and thermodynamic β-sheet propensities of the 20 canonical amino acids have been determined.[3,20−22] β-Branched amino acids, such as valine, isoleucine, and threonine, favored β-sheet structures.[3,20−22] Recently, β-sheets have been studied in the context of protein tertiary folds[23−26] and β-hairpin peptides,[27−34] demonstrating the importance of context, that is, cross-strand interactions, for sheet stability.[27,28,30−34] Furthermore, statistical analysis of protein structures[35−37] also suggested that cross-strand side chain-side chain interactions are important for stabilizing sheet structures. As such, various interactions between two β-strands have been studied, including cation-π,[31,38,39] hydrophobics,[40,41] electrostatics,[40,42−44] van der Waals,[45,46] aromatic π−π,[34,43] and carbohydrate-π.[47]

Protein structures can be stabilized by electrostatic interactions between oppositely charged amino acids.[48,49] Since electrostatic interactions are important for protein stability and such interactions are frequently observed in proteins as ion pairs,[50] the energetics of individual ion pairs has been determined in proteins.[51−54] Oppositely charged amino acids are frequently observed directly across one another in

Received: July 21, 2013
Revised: November 26, 2013
Published: December 12, 2013

   dx.doi.org/10.1021/bi400974x | *Biochemistry* 2013, 52, 9212−9222

antiparallel sheet structures,[35] suggesting specific ion pairing interactions. Accordingly, the energetics of cross-strand ion pairs have been measured in sheet-containing host systems including the protein G B1 domain[26,55] and zinc finger domain.[25] For the protein G B1 domain, a cross-strand lateral Glu-Lys ion pairing interaction increased the stability by 1.0 kcal/mol based on thermal denaturation studies.[26] Individual secondary structures are typically marginally stable, so the quantitative analysis for autonomously folded β-hairpins, the simplest β-sheet motif, is more difficult than sheet-containing tertiary structures. Regardless, the energetics of cross-strand ion pairing in β-haripins has been reported.[31,40,43,44,56,57] In short hairpin peptides, cross-strand lateral Glu-Lys ion pairing interactions provided 0.1−0.3 kcal/mol stability based on NMR methods.[43,44,57] Furthermore, the cross-strand lateral Glu-Lys ion pairing interaction closer to the turn was stronger compared to the same interaction closer to the termini in a hairpin forming peptide,[57] most likely due to end fraying effects.[57] In addition, a cross-strand backbone to side chain ion pairing interaction provided 0.2−0.3 kcal/mol stability in a hairpin peptide based on NMR methods.[58]

Amino acids with positively and negatively charged functionalities participate in protein electrostatic interactions. Interestingly, the canonical charged residues Asp, Glu, Arg, and Lys all contain a different number of methylenes on the side chain. The reason why these particular charged residues were chosen by nature and the role of the linking methylenes in ion pairing interactions remain unclear. Amino acids with the same functionality but different side chain lengths exhibited varying secondary structure propensities.[7,9,59−62] The helix propensity increased as the side chain lengths of Glu and Lys analogues increased.[59−62] The stability of a β-hairpin motif also increased upon increasing the Lys analogue side chain length.[9,39] However, the stability trend for the Asp/Glu analogues varied depending on the system and even position.[9,20−22] Asp and Glu showed similar thermodynamic sheet propensities in a zinc finger domain.[20] Nevertheless, the thermodynamic sheet propensity in the protein G B1 domain increased upon increasing the side chain length from Asp to Glu.[21,22] In short hairpin peptides, the stability trend of carboxylate bearing amino acids is position dependent.[9] The effect of charged amino acid side chain length on intrahelical glutamate-lysine ion pairing interaction has been explored in detail.[6,63] However, the effect of oppositely charged residues side chain length on cross-strand ion pairing interactions in β-hairpins has yet to be systematically studied. Herein, we present a systematic study of a series β-hairpins peptides containing potential cross-strand ion pairs between oppositely charged residues with varying side chain lengths using NMR methods. The interaction energy was determined by double mutant cycle analysis, and a non-redundant protein structure database was surveyed for sequence patterns with oppositely charged residues across one another in antiparallel β-sheets.

MATERIALS AND METHODS

Peptide Synthesis. Peptides were synthesized by solid phase peptide synthesis using Fmoc-based chemistry.[64,65] The disulfide bond of the Cys-containing HPTFZbbXaa peptides was formed via charcoal-mediated air oxidation.[66] All peptides were purified by reverse-phase high performance liquid chromatography to greater than 95% purity. The identity of the peptides was confirmed by matrix-assisted laser desorption ionization time-of-flight mass spectrometry (MALDI-TOF). More detailed procedures and peptide characterization data are provided in the Supporting Information.

Nuclear Magnetic Resonance Spectroscopy. NMR samples were prepared by dissolving the lyophilized purified peptides with purity above 95% into H_2O/D_2O (9:1 ratio by volume) in the presence of 50 mM sodium deuterioacetate buffer, pH 5.5 (uncorrected). Peptide concentrations were 1−10 mM. 2-Dimethyl-2-silapentane-5-sulfonate (DSS) was added to the samples as an internal reference. All NMR experiments were performed on a Brüker AV III 800 MHz spectrometer. Phase-sensitive DQF-COSY,[67] TOCSY,[68] NOESY,[69] and ROESY[70] experiments were performed at 298 K; 2048 points were collected in f2 with 4−8 scans and 256−512 points in f1. Solvent suppression was achieved by the WATERGATE solvent suppression sequence.[71,72] TOCSY and ROESY experiments employed a spin locking field of 10 kHz. A mixing time of 60 ms was used for the TOCSY experiments, 120 ms was used for the NOESY experiments, and 200 ms was used for the ROESY experiments.

Chemical Shift Deviation. Sequence specific assignments for all peptides were completed by using the 2D-NMR spectra (DQF-COSY,[67] TOCSY,[68] NOESY,[69] ROESY[70]). The Hα chemical shift deviation ($\Delta\delta$Hα)[73,74] is the difference between the observed Hα chemical shift (δHα) and the random coil Hα chemical shift. The unfolded reference HPTUZbbXaa peptides were assumed to be random coil.[31] The chemical shift deviation for each residue of the experimental peptide ($\Delta\delta$Hα(exp)) and the folded reference peptide ($\Delta\delta$Hα(F)) were derived using eqs 1 and 2,[74] respectively, where δHα(exp) was the Hα chemical shift from the residue of interest of the experimental peptide, δHα(U) was the Hα chemical shift for the corresponding residue on the unfolded reference peptide, and δHα(F) was the Hα chemical shift from the residue of interest on the folded reference peptide.

$$\Delta\delta\mathrm{H}\alpha(\mathrm{exp}) = \delta\mathrm{H}\alpha(\mathrm{exp}) - \delta\mathrm{H}\alpha(\mathrm{U}) \quad (1)$$

$$\Delta\delta\mathrm{H}\alpha(\mathrm{F}) = \delta\mathrm{H}\alpha(\mathrm{F}) - \delta\mathrm{H}\alpha(\mathrm{U}) \quad (2)$$

Interproton Distances from NOE Cross Peaks. The NOE cross peaks for all peptides were assigned from the corresponding ROESY spectra. The intensity of each NOE cross peak was measured by the integration based on a Gaussian peak model. The distance between the two β hydrogen atoms on the proline side chain (regardless of stereochemistry) was set as the standard (1.77 Å) to derive the interproton distance for the cross peak of interest using eq 3.[75] The distances (R_{residue}) were grouped into short (≤2.5 Å), medium (2.5−3.5 Å), and long (>3.5 Å) for the depictions in the Wüthrich diagrams (Figures S15−S26, Supporting Information).

$$R_{\mathrm{residue}} = 1.77 \times 10^{-10} \times \left(\frac{I_{\mathrm{standard}}}{I_{\mathrm{residue}}}\right)^{1/6} \quad (3)$$

Fraction Folded Population and Folding Free Energy (ΔG_{fold}). The fraction folded population and folding free energy (ΔG_{fold}) for each residue were derived from Hα chemical shift values assuming a two-state folding model for the β-hairpin peptides.[31,76] The fraction folded population for a given residue was derived using eq 4,[31,76] where δHα(exp) was the Hα chemical shift of the residue of interest on the experimental peptide, δHα(U) was the Hα chemical shift of the corresponding residue on the unfolded reference peptide, and

dx.doi.org/10.1021/bi400974x | Biochemistry 2013, 52, 9212−9222

$\delta H\alpha(F)$ was the $H\alpha$ chemical shift of the corresponding residue on the folded reference peptide. The folding free energy (ΔG_{fold}) for each residue was derived using eq 5.[31,76] The fraction folded population and ΔG_{fold} of each peptide were determined by averaging the corresponding values for residues at positions 2, 3, 9, and 10. For comparing the folding free energy or fraction folded population, the values were considered to be different if the Z value was greater than 0.67 (which should give a P value of 0.5 or less considering a two-tailed model).

$$\text{fraction folded population} = \frac{\delta H\alpha(\text{exp}) - \delta H\alpha(U)}{\delta H\alpha(F) - \delta H\alpha(U)} \times 100\% \quad (4)$$

$$\Delta G_{fold} = -RT \ln \frac{\delta H\alpha(\text{exp}) - \delta H\alpha(U)}{\delta H\alpha(F) - \delta H\alpha(\text{exp})} \quad (5)$$

$^3J_{NH\alpha}$ Spin−Spin Coupling. The peak-to-peak separation in the absorptive (ν_a) and dispersive (ν_d) DQF-COSY spectra was measured to derive the $^3J_{NH\alpha}$ coupling constant based on the values along the f2 axis unless there was significant spectral overlap. The dispersive spectrum is a 90° phase shift from the absorptive antiphase spectrum. Since the $H\alpha$ has passive coupling caused by $H\beta$, the passive coupling may cause inaccuracy in the derivation of the $^3J_{NH\alpha}$ values. Accordingly, the peak separation was measured at the NH region. The absorptive (ν_a) and dispersive (ν_d) values were used to derive the $^3J_{NH\alpha}$ coupling constant from the square root of the single real root using eq 6.[77]

$$J^6 - \nu_d^2 J^4 + \left(-\frac{9}{4}\nu_a^4 + \frac{3}{2}\nu_a^2\nu_d^2 + \frac{3}{4}\nu_d^4\right)J^2 + \frac{81}{64}\nu_a^6 - \frac{9}{16}\nu_a^4\nu_d^2 - \frac{21}{32}\nu_a^2\nu_d^4 - \frac{1}{16}\nu_d^6 + \frac{\nu_d^8}{64\nu_a^2} = 0 \quad (6)$$

Double Mutant Cycle Analysis. Double mutant cycle analysis was performed to determine the interaction free energy (ΔG_{int}) between charged residues Zbb and Xaa in the HPTZbbXaa peptides using eq 7.[78,79] This analysis accounted for the effect of each charged residue (individually) on strand stability using data from the corresponding Ala-containing peptides HPTZbbAla and HPTAlaXaa (Tables 1 and S49)[9] to determine the Zbb-Xaa ion-pairing interaction exclusively. The peptide with Ala incorporated at positions 4 and 9, HPTAlaAla, was used as the reference peptide.

$$\Delta G_{int} = (\Delta G_{HPTZbbAla} - \Delta G_{HPTAlaAla}) - (\Delta G_{HPTAlaXaa} - \Delta G_{HPTAlaAla}) - (\Delta G_{HPTZbbXaa} - \Delta G_{HPTAlaAla}) \quad (7)$$

Survey of β-Sheet Residues in Natural Proteins. The survey was performed on the PDBselect (April 2009, 25% threshold),[80,81] a database of nonredundant protein chains. The β-strand conformation, strand orientation (i.e., parallel and antiparallel), context (i.e., internal and edge strand, non-hydrogen bonded and hydrogen bonded positions), and relative residue positioning (lateral and diagonal) was defined based on DSSP.[82,83] The corresponding sheet residues of interest were selected, and the occurrences were compiled using in-house code written in ActivePerl 5.8.8.819. The statistical propensity of a given amino acid type for a given β-sheet structural context was derived by dividing the occurrence of the given amino acid type in the given β-sheet structural context by the expected occurrence based on all structures in the database. The expected occurrence and the corresponding standard deviation were obtained by bootstrapping[84] the β-sheet structural context against the entire PDBselect database. The bootstrapping was performed by running in-house code written in C++ using the high-performance computing facilities in the Computer and Information Networking Center at National Taiwan University. Dividing the difference between the occurrence and the expected occurrence by the standard deviation gave the Z value, which was used to obtain the P value based on a normal distribution.[85,86] The P values were obtained using the program R 2.15.2 (64-bit) on a MacBookPro (2.3 GHz Intel Core I5) running MacOSX10.7.5.

RESULTS

Peptide Design and Synthesis. The sequences for the experimental HPTZbbXaa were designed based on peptide YKL (Figure 1),[31,76,87] which exhibited 68% β-hairpin fraction

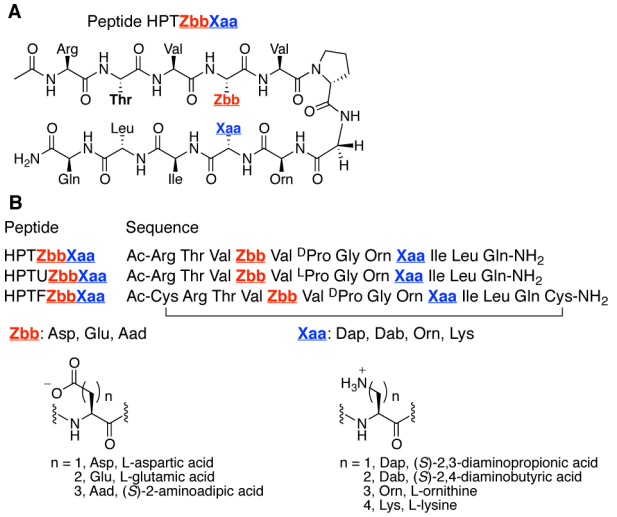

Figure 1. Design of peptides to study the effect of charged amino acid side chain length on lateral ion pairing interactions. Panel A: the chemical structure of the experimental HPTZbbXaa peptides. Panel B: the sequences of the experimental HPTZbbXaa peptides, the unfolded reference HPTUZbbXaa peptides, and the folded reference HPTFZbbXaa peptides.

folded population,[31,76,87] as originally designed by Gellman and co-workers.[31,76,87] Ornithine was included to avoid aggregation and maintain the residue diversity to distinguish the signal from lysine in NMR analysis.[31] The DPro-Gly was designed to form a two-residue loop for the β-hairpin conformation.[87] The Tyr2 (in peptide YKL) was mutated to Thr to avoid the diagonal Lys9-Tyr2 cation-π interaction, but should not significantly affect the hairpin conformation due to similar sheet propensities for Tyr and Thr. The N- and C-termini were capped by an acetyl group and carboxyamide, respectively, to minimize unintended electrostatic interactions involving the charged termini.[40] To study the effect of charged amino acid side chain length on cross-strand lateral ion pairing interactions, various negatively charged and positively charged residues were incorporated at positions 4 and 9, respectively. Positions 4 and 9 are inward pointing non-hydrogen bonded positions on the N- and C-terminal strands, respectively. These two positions

dx.doi.org/10.1021/bi400974x | Biochemistry 2013, 52, 9212−9222

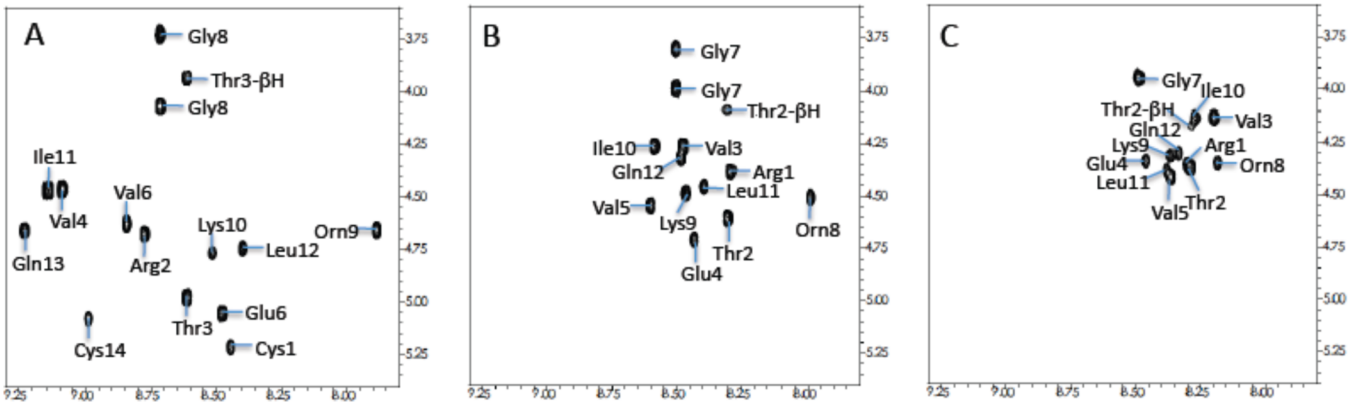

Figure 2. The Hα-HN region of the TOCSY spectra for peptides HPTFGluLys (A), HPTGluLys (B), and HPTUGluLys (C).

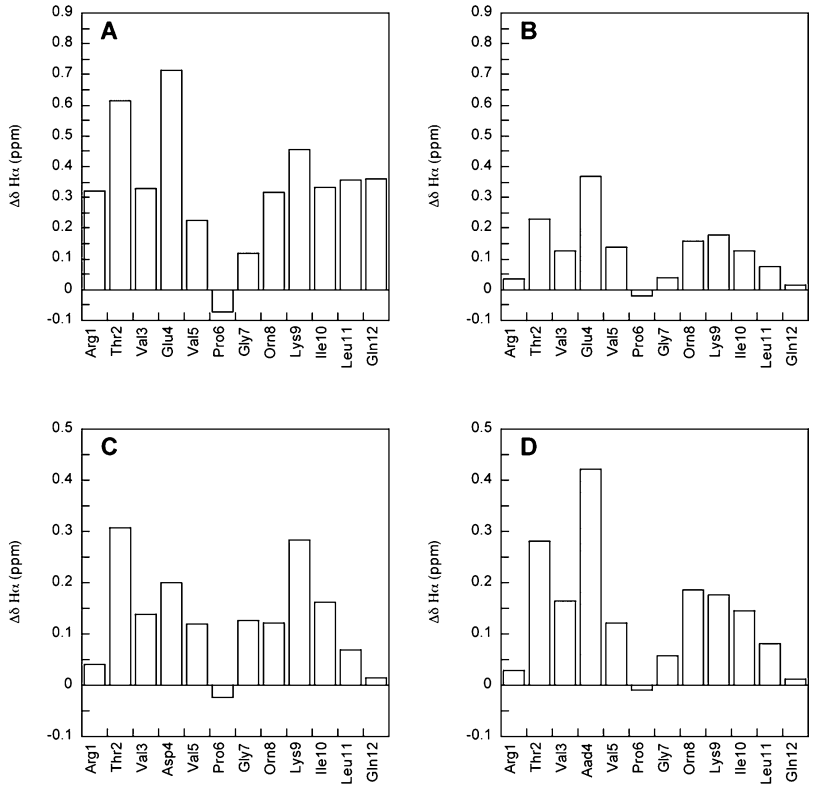

Figure 3. The chemical shift deviation ($\Delta\delta$Hα) for the residues in peptides HPTFGluLys (A), HPTGluLys (B), HPTAspLys (C), and HPTAadLys (D).

are near the center of the β-strands to avoid end fraying effects.[88] Besides, the potential ion pair were not too close to the turn; otherwise, the ion pairing interaction could be artificially amplified.[43,88] The negatively charged residue Zbb was systematically lengthened from Asp (one methylene) to Glu (two methylenes) and then to (*S*)-2-aminoadipic acid (Aad, three methylenes) (Figure 1B). The positively charged residues Xaa was systematically shortened from Lys (4 methylenes) to Orn (3 methylenes), (*S*)-2,4-diaminobutyric acid (Dab, 2 methylenes), and (*S*)-2,3-diaminopropionic acid (Dap, 1 methylene) (Figure 1B). Fully unfolded and folded reference peptides were necessary to determine the fraction folded population for the experimental HPTZbbXaa peptides.[31,34,38,76] The unfolded reference peptides HPTUZbbXaa were designed by changing the turn sequence from D-Pro to L-Pro (Figure 1B) and were presumed to be fully unfolded because this change has been shown to disrupt the β-hairpin conformation.[76,89] The folded reference peptides HPTFZbbXaa were designed by introducing cysteines at both the N- and C-terminus for cyclization via disulfide bond formation (Figure 1B),[31,34,38,76] and were presumed to be fully folded. The peptides were named according to the one-letter code of the mutated residues and the three-letter code of the negatively and positively charged residues. For example, the peptide of HPTUZbbXaa is a ***H***air***P***in peptide with Tyr2 replaced with ***T***hr2, DPro6 replaced with Pro for the ***U***nfolded reference peptides, and Zbb and Xaa at positions 4 and 9, respectively.

The peptides were synthesized by solid phase peptide synthesis using Fmoc-based chemistry.[64,65] The disulfide bond of the folded reference HPTFZbbXaa peptides was formed via charcoal mediated air oxidation.[66] All peptides were purified by reverse-phase high performance liquid chromatography to

dx.doi.org/10.1021/bi400974x | *Biochemistry* 2013, 52, 9212−9222

greater than 95% purity and confirmed by MALDI-TOF. Since the NMR spectra (chemical shift and line width) of analogous hairpin peptides did not change with concentration (20 μM to 10 mM),[9,27,31,90] the peptides in this study (1.5−12.4 mM) should not aggregate in solution. Accordingly, the experimental data should reflect the intramolecular interactions with minimal interference from intermolecular interactions.

β-Hairpin Structure Characterization by NMR. The peptides were analyzed by two-dimensional NMR spectroscopy including total correlation spectroscopy (TOCSY),[68] double-quantum filtered-correlated spectroscopy (DQF-COSY),[67] two-dimensional nuclear Overhauser spectroscopy (NOESY),[69] and rotating frame nuclear Overhauser spectroscopy (ROESY)[70] at 298 K. Sequence specific assignments of the chemical shifts were performed based on the TOCSY and ROESY spectra (Tables S1−S36, Supporting Information).[91] In general, the folded reference HPTFZbbXaa peptides showed higher chemical shift dispersion compared to the corresponding experimental HPTZbbXaa peptides; the corresponding unfolded reference HPTUZbbXaa peptides displayed the lowest chemical shift dispersion (Figure 2 and Tables S1−S36). These chemical shift dispersion trends were consistent with the expected fraction folded populations; the higher the fraction folded population, the higher the chemical shift dispersion.[92] Also, the extent of chemical shift dispersion of the experimental HPTZbbXaa peptides reflected the relative fraction folded populations.

The hairpin structure of the experimental HPTZbbXaa peptides and the folded reference HPTFZbbXaa peptides were confirmed by Hα chemical shift deviations ($\Delta\delta$Hα),[73,74] $^3J_{NH\alpha}$ spin−spin coupling constants, and cross-strand NOEs. The $\Delta\delta$Hα values for the residues in the experimental peptides HPTZbbXaa and folded reference peptides HPTFZbbXaa were derived using the δHα of the residues in the unfolded reference HPTUZbbXaa peptides as the random coil values[31] (Figures 3, S1, and S2). For a residue at a strand position, the Hα chemical shift should display a downfield shift in a β-sheet conformation compared to the same residue in the corresponding unfolded reference peptide, and give a positive $\Delta\delta$Hα value.[74] For the HPTZbbXaa and HPTFZbbXaa peptides, residues Thr2 through Val5 and Orn8 through Leu11 exhibited significantly positive $\Delta\delta$Hα values (Figures 3, S1, and S2), suggesting that these peptides displayed a reasonable β-hairpin population. The $\Delta\delta$Hα values of the terminal residues Arg1 and Gln12 were near zero, which is typically observed for the terminal residues in a β-hairpin construct due to end fraying effects.[88] The $\Delta\delta$Hα values for DPro6 and Gly7 were mostly close to zero, suggesting turn formation.[27] Importantly, the folded reference peptides expectedly exhibited higher $\Delta\delta$Hα values compared to the corresponding experimental peptides (Figures 3, S1, and S2), indicating that the folded reference HPTFZbbXaa peptides were more well folded compared to the corresponding experimental HPTZbbXaa peptides.

The $^3J_{NH\alpha}$ spin−spin coupling constant for the residues in the peptides was derived from the DQF-COSY spectra.[77] A $^3J_{NH\alpha}$ value less than 6 Hz for a residue is considered to adopt an α-helical conformation,[91] whereas a $^3J_{NH\alpha}$ value greater than 7 Hz is considered to be in a β-sheet conformation.[91] In the folded reference HPTFZbbXaa peptides, the $^3J_{NH\alpha}$ values for all residues except the cysteines and glycine were higher than 7 Hz (Tables S40−S42, Supporting Information), consistent with a β-sheet conformation.[91] The experimental HPTZbbXaa peptides exhibited similar results but slightly lower $^3J_{NH\alpha}$ values for some residues (Tables S43−S45, Supporting Information). Although this suggested that these peptides form a β-hairpin conformation, the structure may not be as well-defined as the folded reference peptides. Regarding the unfolded reference HPTUZbbXaa peptides, some residues exhibited $^3J_{NH\alpha}$ values near to or less than 7 Hz, suggesting that the peptides might not form a well-defined β-hairpin or α-helical conformation and are thus most likely unfolded (Tables S46−S48, Supporting Information).

Cross-strand NOE connectivities obtained from the ROESY spectra further supported β-hairpin formation. The NOE cross peaks including sequential, intraresidues, medium range, and long-range NOEs with a number of cross-strand Hα ↔ Hα, Hα ↔ NH, NH ↔ NH correlation confirmed the peptide conformation (Figures S3−S26, Supporting Information). The β-strand structures were confirmed by diagnostic NOEs. The network of side chain-side chain NOEs between residues on the two adjacent β-strands further confirmed β-hairpin formation for the experimental peptides HPTZbbXaa and folded reference peptides HPTFZbbXaa (Figures S3−S14, Supporting Information). The side chain of Thr2 exhibited lateral hydrophobic contacts to the Leu11 residue, especially in the folded reference peptides HPTFZbbXaa (Figures S3−S14). The side chain of the two oppositely charged residues Zbb4 and Xaa9 also showed cross-strand NOE connectivities to one another in some cases (Figures S3−S14, Supporting Information). Interestingly, the distinct NOE cross-peaks between Thr2 and Xaa9 were clearly observed in the experimental HPTZbbXaa peptides (Figures S3−S14). Thr2 appears to be far from Xaa9 in a flat structure, however the typical right-handed twist of β-hairpin structures gives rise to these long-range diagonal cross-strand NOE connectivities (Figures S3−S14).[27,31,75,76] The number of cross peaks in the ROESY spectra followed the trend HPTFZbbXaa > HPTZbbXaa > HPTUZbbXaa (Figures S3−S26, Supporting Information). This trend was consistent with the intended fraction folded population for the peptides.

Fraction Folded Population and ΔG_{fold}. The fraction folded population and folding free energy (ΔG_{fold}) for each residue on the experimentatal HPTZbbXaa peptides were determined from the Hα chemical shift data (Tables 1 and S49, and Figure 4). The fraction folded population of the residues at the N- and C-termini was very low, most likely due to end fraying effects (Figure S27, Supporting Information). On the contrary, the residues directly adjacent to the turn exhibited high fraction folded population (Figure S27), which should be due to turn-promoted sheet formation. Accordingly, residues

Table 1. The Fraction Folded Population (%) for the HPTZbbXaa Peptides[a,b]

	Zbb			
Xaa	Ala	Asp	Glu	Aad
Ala	16 ± 4	37 ± 1[c]	29 ± 2[c]	25 ± 2[c]
Dap	16 ± 1[c,d]	55 ± 3	63 ± 2	25 ± 1
Dab	14 ± 3[c]	35 ± 4	24 ± 2	26 ± 2
Orn	21 ± 3[c]	48 ± 2	38 ± 2	42 ± 3
Lys	22 ± 3[c]	52 ± 3	38 ± 1	44 ± 4

[a]The general sequence for the HPTZbbXaa peptides is Ac-Arg-Thr-Val-Zbb-Val-DPro-Gly-Orn-Xaa-Ile-Leu-Gln-NH_2. [b]Average value for residues 2, 3, 9, and 10. [c]Values have been previously determined using the same method.[9] [d]Average value for residues 2, 3, and 10.

dx.doi.org/10.1021/bi400974x | Biochemistry 2013, 52, 9212−9222

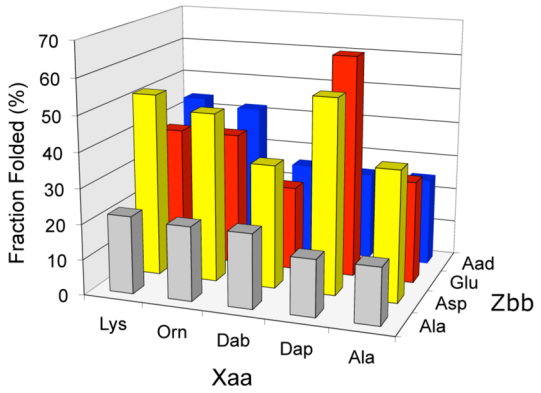

Figure 4. The fraction folded population for HPTZbbXaa peptides.

Thr2, Val3, Xaa9, and Ile10 were chosen to represent the fraction folded population for a given peptide (Table 1; Figures 4 and S27). These residues were selected to also provide equal representation for the hydrogen bonded (3 and 10) and non-hydrogen bonded positions (2 and 9) on the two strands and account for the apparent uneven folding of the two strands due to the inherent right-handed twist.

The fraction folded populations for HPTZbbXaa peptides with charged residues at both guest positions were between 24% and 63%, and the standard deviations were within 5% (Table 1 and Figure 4). For a given negatively charged residue, the fraction folded population seemed to roughly increase with increasing side chain length of the positively charged residue, except for the shortest residue Dap. This trend was consistent with the sheet propensity of the positively charged residue Xaa: Lys > Orn >Dab.[39] Peptides containing Dab (two methylenes) exhibited the least fraction folded population for a given negatively charged residue. Interestingly, the HPTAspXaa and HPTGluXaa peptides containing the shortest positively charged residue Dap showed exceptionally high fraction folded population. In particular, peptide HPTGluDap exhibited the highest fraction folded population for all peptides. In contrast, among the HPTAadXaa peptides, the peptide with the shortest residue Dap (HPTAadDap) exhibited the least fraction folded population, which was similar to the fraction folded population for HPTAadDab. Interestingly, this result mirrors the stability of the peptides with the positively charged residues at the C-terminal non-hydrogen bonded guest position 9 (and Ala at position 4), which followed the trend: Dap ~ Dab < Orn ~ Lys (Table S49).[9]

Lateral Cross-Strand Zbb−Xaa Interactions. The interaction free energy (ΔG_{int}) for each lateral Zbb-Xaa interaction between oppositely charged residues was derived from the corresponding double mutant cycle (Table 2).[78,79] The ΔG_{int} values for cross-strand lateral Zbb-Xaa ion pairing interactions were mostly nonexistent (Table 2). However, the interaction energy between two residues is a relative but not absolute value between one state and another state.[78] Therefore, a zero interaction free energy ($\Delta G_{int} = 0$) only indicates no variation in coupling energy between charged residues Zbb and Xaa from one state to another but does not mean they are not coupled to each other.[78] Importantly, four cross-strand lateral ion pairing interactions were clearly stabilizing: Glu-Dap, Asp-Dap, Aad-Lys, and Aad-Orn. The natural amino acid Glu exhibited the most stabilizing interaction energy for Zbb-Dap followed by the natural amino acid Asp. However, the residue Aad provided the highest stabilizing interaction energy for the Zbb-Lys and Zbb-Orn lateral cross-strand interactions for the given positively charged residues Lys and Orn, respectively. Interestingly, both oppositely charged residues with short side chain lengths formed the more stabilizing ion pairs Asp-Dap and Glu-Dap compared to the longer side chain pairs Aad-Lys and Aad-Orn. As such, the short side chain lengths for oppositely charged residues with lateral cross-strand arrangements may provide a more well-defined interaction to stabilize the β-hairpin structure compared to the long side chain lengths. Importantly, the longest negatively charged residue Aad paired with the longer positively charged residues Lys and Orn, and the shorter negatively charged residues Glu and Asp paired with the shortest positively charged residue Dap. This suggests that side chain length matching of the oppositely charged residues is important for forming stabilizing lateral cross-strand interactions.

Table 2. Zbb-Xaa Interaction Free Energy (ΔG_{int}, kcal/mol) in HPTZbbXaa Peptides

	Zbb		
Xaa	Asp	Glu	Aad
Dap	**−0.41 ± 0.19**	**−0.83 ± 0.19**	−0.02 ± 0.19
Dab	−0.02 ± 0.22	0.07 ± 0.22	−0.14 ± 0.22
Orn	−0.07 ± 0.20	−0.06 ± 0.21	**−0.28 ± 0.22**
Lys	−0.11 ± 0.20	−0.02 ± 0.20	**−0.29 ± 0.23**

DISCUSSION

The effect of side chain length on lateral ion pairing interactions between carboxylate and ammonium amino acids at non-hydrogen bonded positions on different strands of a β-hairpin was investigated. The fraction folded population for peptide HPTGluLys (Table 1, 38 ± 1%) was significantly lower compared to the fraction folded population for the parent YKL peptide (H-Arg-Tyr-Val-DPro-Gly-Orn-Lys-Ile-Leu-Gln-NH_2, 68%),[31] most likely due to the loss of the cross-strand diagonal Lys-Tyr cation-π interaction and the lateral Tyr-Leu hydrophobic interaction. However, the fraction folded population for peptide HPTGluLys (Table 1, 38 ± 1%) was similar to the fraction folded population for the analogous VKL peptide (Ac-Arg-Val-Val-Glu-Asn-Gly-Orn-Lys-Ile-Leu-Gln-NH_2, 37%),[39] showing similar characteristics upon substituting Val with Thr.

The fraction folded population for all HPTZbbXaa peptides with charged residues at both guest positions was between 24% and 63% (Table 1). This extensive range for the fraction folded population can be rationalized by considering several factors including the sheet/strand propensity of the individual Lys and Glu analogues, the diagonal Thr2-Xaa9 hydrophobic interaction, and the lateral Zbb4-Xaa9 hydrophobic and electrostatic interactions. The fraction folded populations of the peptides HPTAspDap, HPTGluDap, and HPTAadDap were 55%, 63%, and 25%, respectively (Table 1 and Figure 4). Since the ROESY spectra for all three peptides exhibited NOEs cross-peaks between Thr2 and Dap9 (Figures S3B, S7B, S11B, Supporting Information), the Thr2-Dap9 diagonal interactions should be similar for these three peptides. Therefore, the difference in the fraction folded population for these three peptides should be due to the sheet/strand propensity of the negatively charged residue, and the lateral Zbb4-Dap9 hydrophobic and electrostatic interactions. The effect of the negatively charged residue side chain length at the non-hydrogen bond guest position 4 on

dx.doi.org/10.1021/bi400974x | Biochemistry 2013, 52, 9212−9222

Table 3. Survey Results on Lateral Antiparallel Cross-Strand Sequence Patterns[a]

position i	position j	context[b]	strand context[a]	no.[a]	sheet pair propensity[c]	Z value	P value	salt bridge[d]
Asp	Lys	NHB−NHB	internal−internal	21	0.37 ± 0.05	−4.83	1.38×10^{-6}	5
Glu	Lys	NHB−NHB	internal−internal	83	1.23 ± 0.15	1.90	5.79×10^{-2}	6
Asp	Lys	HB−HB	internal−internal	30	0.51 ± 0.07	−3.77	1.64×10^{-4}	2
Glu	Lys	HB−HB	internal−internal	99	1.44 ± 0.17	3.62	2.97×10^{-4}	10
Asp	Lys	NHB−NHB	edge−edge	84	1.40 ± 0.18	3.10	2.00×10^{-3}	23
Glu	Lys	NHB-NHB	edge−edge	133	1.88 ± 0.22	7.44	9.96×10^{-14}	8
Asp	Lys	HB−HB	edge−edge	64	1.05 ± 0.14	0.42	6.74×10^{-1}	2
Glu	Lys	HB−HB	edge−edge	115	1.61 ± 0.19	5.20	1.95×10^{-7}	5
Asp	Lys	NHB−NHB	internal−edge	22	0.30 ± 0.03	−6.05	1.42×10^{-9}	3
Glu	Lys	NHB−NHB	internal−edge	99	1.14 ± 0.12	1.35	1.78×10^{-1}	6
Asp	Lys	HB−HB	internal−edge	50	0.69 ± 0.08	−2.67	7.61×10^{-3}	1
Glu	Lys	HB−HB	internal−edge	126	1.48 ± 0.16	4.44	8.88×10^{-6}	6
Asp	Lys	NHB−NHB	edge−internal	65	0.88 ± 0.10	−1.01	3.14×10^{-1}	20
Glu	Lys	NHB−NHB	edge−internal	136	1.57 ± 0.17	5.32	1.04×10^{-33}	12
Asp	Lys	HB−HB	edge−internal	53	0.73 ± 0.08	−2.36	1.82×10^{-2}	2
Glu	Lys	HB−HB	edge−internal	149	1.75 ± 0.19	6.97	3.07×10^{-12}	5

[a]The occurrence of oppositely charged residues on antiparallel neighboring strands in the nonredundant protein structure database PDBselect (April 2009, 25% threshold).[80,81] The β-strand conformation was defined based on DSSP.[82,83] The residues on an internal strand and an edge strand were defined based on the presence of complementary strands on both sides and on only onside using DSSP, respectively.[82,83] The antiparallel and parallel orientations were defined based on DSSP.[82,83] [b]The non-hydrogen bonded (NHB) and hydrogen bonded (HB) residues were defined based on the hydrogen bond definition using DSSP.[82,83] [c]The occurrence for the various sequence patterns divided by the corresponding expected value. The expected value was obtained by bootstrapping the complete PDBselect database, thereby including the bias for the occurrence of each residue for the sheet conformation. Since bootstrapping was performed 100,000 times, this enabled the calculation of a standard deviation for the expected value and thus the sheet pair propensity. [d]The number of the occurrences for each sequence pattern that actually forms salt bridges between the oppositely charged side chain functionalities. The presence of a salt bridge is defined by an N−O distance less than or equal to 3 Å.

β-hairpin stability followed the trend: Asp > Glu > Aad (Table 1).[9] However, the fraction folded population of the HPTZbbDap peptides did not strictly follow this trend (Table 1 and Figure 4), suggesting that the lateral interactions between the side chains of Zbb4 and Dap9 do contribute to the β-hairpin stability in this case.

The fraction folded population decreased significantly from 63% to 24% upon adding a methylene to the Dap side chain in peptide HPTGluDap to give peptide HPTGluDab (Table 1 and Figure 4). Evidently, this result does not mirror the effect of the positively charged residue side chain length at the non-hydrogen bonded guest position 9 on β-hairpin stability: Dab ≥ Dap (Table 1).[9] As such, this might be caused by a stronger Thr2-Dap9 diagonal interaction compared to Thr2-Dab9, as evidenced by the number of NOE connectivities (Figures S7B and S8B, Supporting Information) or might caused by a more stabilizing lateral Glu4-Dap9 interaction compared to the Glu4-Dab9 interaction (Table 2).

Intrahelical ion pairing interactions can contribute up to −0.8 kcal/mol to helix stability.[63,93] In β-hairpin peptides, ion pairing interactions provide −0.1 to −0.4 kcal/mol stability.[40,42−44,57] The energetic contribution of lateral ion pairs to peptide stability in our study was determined by double mutant cycle analysis (Table 2), and the values were mostly consistent with previous reports. Interestingly, both Glu-Dap and Asp-Dap pairs, which have a canonical negatively charged residue, contributed the most stability to the hairpin. In particular, the lateral Glu-Dap interaction provided −0.83 kcal/mol to the hairpin stability (Table 2).

The least number of methylenes would provide the most side chain rigidity, leading to a strong lateral Asp-Dap ion pairing interaction due to minimal entropic penalty upon forming an ion pair. However, increasing the positively or negatively charged residues by one methylene to Asp-Dab or Glu-Dap ion pairs gave drastically different results. The lateral Glu-Dap interaction contributed more to the β-hairpin stability compared to the Asp-Dap interaction. In contrast, the Asp-Dab pair contributed less to the β-hairpin stability compared to the Asp-Dap pair. As such, hydrophobics should not dominate the Glu-Dap and Asp-Dab interaction energetics, because increasing the side chain length should increase the hydrophobics for both cases. Instead, lengthening Asp by one methylene to Glu would increase the electron-donating characteristics, decrease the electron-withdrawing characteristics from the backbone functionality and thus raise the anionic charge density on the carboxylate group, enhancing the electrostatic interaction with the positively charged Dap. On the other hand, increasing the side chain length of Dap by one methylene to give Dab would decrease the cationic character on the ammonium group, thereby decreasing the electrostatic interaction with the negatively charged Asp. Taking this discussion another step further, increasing the side chain length of Asp by two methylenes to give the Aad-Dap ion pair removed the favorable ion pairing interaction altogether. Although the two extra methylenes should donate more electron density to the carboxylate and withdraw less electron density from the carboxylate, the longer side chain would also provide more flexibility and increase the entropic penalty upon forming an ion pair, resulting in the nonexistent interaction energy. In order to optimize the Aad-Dap ion pairing interaction, the conformation would be constrained with high entropic penalty, lowering the overall energetic contribution to β-hairpin stability.

The energetics of the Aad-Orn/Lys interactions was more stabilizing compared to the Glu-Orn/Lys interactions, even though the negatively charged residue Aad was only one methylene longer than Glu. Apparently, the longer Aad side chain with more methylenes can interact through hydrophobics and can also serve as an electron-donating group for the carboxylate group, or as a spacer to separate the electron-

withdrawing backbone from the carboxylate, to enable stronger electrostatic interactions with the positively charged residues.

Lengthening the positively charged residue in the Aad-Dap/Dab ion pairs gave the more stabilizing Aad-Orn/Lys ion pairs. The longer positively charged residues Orn/Lys would provide more hydrophobicity and flexibility for the side chain compared to the shorter residues Dap/Dab. The contribution of electrostatics (to the interaction energy) would decrease and hydrophobics would increase as the side chain length for the positively charged residues increases. Accordingly, the main contribution to the lateral Zbb-Xaa cross-strand ion pairing interaction was apparently electrostatics for the shorter side chains (Asp/Glu-Dap) and hydrophobics for the longer side chains (Aad-Orn/Lys). Importantly, length matching for the oppositely charged residues appeared to be critical for providing stabilizing energetics for β-hairpin structures. Nevertheless, the positively charged residues with a guanidinium group (Agp, Agb, Arg, Agh) should provide different effects because the effect of side chain length has been shown to be different.[7,9]

A survey was performed on the nonredundant protein structure database PDBselect (April 2009, 25% threshold)[80,81] to study the structural sequence patterns that may support lateral cross strand Asp-Lys and Glu-Lys interactions in β-sheets in naturally proteins (Table 3). A total of 4418 protein chains involving 666 086 residues were considered, and there were 150 934 β-sheet residues. The sheet pair propensity represents how frequently a particular sequence pattern occurs in a sheet conformation compared to all structures in the database. The sheet pair propensity for each sequence pattern was derived from the expected occurrence in all structures. The survey was performed for antiparallel strands in the β-sheets of natural proteins (Table 3). The lateral sheet pair propensity in antiparallel strands consistently exhibited the trend Glu-Lys > Asp-Lys regardless of context (edge or internal strands, non-hydrogen bonded or hydrogen-bonded positions) (Table 3), suggesting the importance of length matching. However, the number of salt bridges varied depending on context. Since our experimental studies have focused on a β-hairpin motif with potential ion pairs involving only antiparallel orientation with edge strands at non-hydrogen bonded positions, the survey was also narrowed to non-hydrogen bonded positions on edge strands in antiparallel sheets. The statistical sheet pair propensity at non-hydrogen bonded positions on edge strands in antiparallel sheets followed the trend Asp-Lys < Glu-Lys, suggesting the importance of length matching. Although the occurrence of the Asp-Lys pair with the negatively charged residue on the edge strand at non-hydrogen bonded positions was less than the Glu-Lys pair, the number of salt bridges for the Asp-Lys pair was higher than the Glu-Lys pair. Also, clearly favorable (i.e., greater than unity) sheet pair propensity for Asp-Lys was only observed between edge strands at non-hydrogen bonded positions, whereas favorable sheet pair propensity for Glu-Lys was present regardless of context (Table 3). Importantly, the statistical sheet pair propensity trends appeared to suggest the importance of length matching for the oppositely charged residues at non-hydrogen bonded positions on edge strands with antiparallel orientation.

CONCLUSION

The effect of varying the charged amino acid side chain length on ion pairing interactions at lateral non-hydrogen bonded positions on the two strands in a β-hairpin has been studied. Combinations with shorter side chains for both charged residues such as Asp/Glu-Dap ion pairs and longer side chains for both charged residues such as Aad-Orn/Lys ion pairs stabilized the β-hairpin structure. The shorter Asp/Glu-Dap interactions exhibited stabilizing energetics most likely due to electrostatics interaction, whereas the longer Aad-Orn/Lys interactions were stabilizing most likely due to hydrophobics. As such, side chain length matching for the oppositely charged residues on separate strands appears to be important for providing stabilizing energetics in β-hairpin structures. The survey on natural proteins revealed that the sheet pair propensity followed the trend Asp-Lys < Glu-Lys, again suggesting the need for length matching of the lateral interacting residues. These results should facilitate the modulation of β-sheet structure stability by using charged residues with varying side chain lengths, and should be useful in designing stable sheet structures and developing β-hairpin based materials for biomedical applications.

ASSOCIATED CONTENT

Supporting Information

Materials and methods section with details of the synthesis and characterization of the peptides, chemical shift assignment data, chemical shift deviation data, coupling constant data, diagrams indicating NOE connnectivities, fraction folded data, and ΔG_{fold} data. This material is available free of charge via the Internet at http://pubs.acs.org.

AUTHOR INFORMATION

Corresponding Author

*Phone: +886-2-33669789. Fax: +886-2-33668671. E-mail: rpcheng@ntu.edu.tw.

Funding

This work was supported by National Taiwan University (R.P.C.) and the National Science Council in Taiwan (S.J.H., NSC-100-2731-M-002-002-MY2; R.P.C., NSC-99-2113-M-002-002-MY2, NSC-101-2113-M-002-006-MY2).

Notes

The authors declare no competing financial interest.

ACKNOWLEDGMENTS

The authors would like to thank the Computer and Information Networking Center at National Taiwan University for the support of the high-performance computing facilities.

ABBREVIATIONS

Aad, (*S*)-aminoadipate; Ala, alanine; Arg, arginine; Asp, aspartate; Dab, (*S*)-2,4-diaminobutyric acid; Dap, (*S*)-2,3-diaminopropionic acid; DQF-COSY, double-quantum filtered-correlated spectroscopy; Fmoc, *N*-9-fluorenylmethyloxycarbonyl; Glu, glutamate; Lys, lysine; MALDI-TOF, matrix-assisted laser desorption ionization time-of-flight; NMR, nuclear magnetic resonance spectroscopy; NOESY, nuclear Overhauser effect spectroscopy; Orn, ornithine; ROESY, rotating-frame nuclear Overhauser effect spectroscopy; TOCSY, total correlation spectroscopy

REFERENCES

(1) Baldwin, R. L., and Rose, G. D. (1999) Is protein folding hierarchic? I. Local structure and peptide folding. *Trends Biochem. Sci.* *24*, 26−33.

(2) Baldwin, R. L., and Rose, G. D. (1999) Is protein folding hierarchic? II. Folding intermediates and transition states. *Trends Biochem. Sci. 24*, 77−83.
(3) Chou, P. Y., and Fasman, G. D. (1974) Conformational parameters for amino acids in helical, β-sheet, and random coil regions calculated from proteins. *Biochemistry 13*, 211−222.
(4) Donald, J. E., Kulp, D. W., and DeGrado, W. F. (2011) Salt bridges: Geometrically specific, designable interactions. *Proteins 79*, 898−915.
(5) Cheng, R. P., Girinath, P., Suzuki, Y., Kuo, H.-T., Hsu, H.-C., Wang, W.-R., Yang, P.-A., Gullickson, D., Wu, C.-H., Koyack, M. J., Chiu, H.-P., Weng, Y.-J., Hart, P., Kokona, B., Fairman, R., Lin, T.-E., and Barrett, O. (2010) Positional effects on helical Ala-based peptides. *Biochemistry 49*, 9372−9384.
(6) Cheng, R. P., Wang, W.-R., Girinath, P., Yang, P.-A., Ahmad, R., Li, J.-H., Hart, P., Kokona, B., Fairman, R., Kilpatrick, C., and Argiros, A. (2012) Effect of glutamate side chain length on intrahelical glutamate-lysine ion pairing interactions. *Biochemistry 51*, 7157−7172.
(7) Cheng, R. P., Weng, Y.-J., Wang, W.-R., Koyack, M. J., Suzuki, Y., Wu, C.-H., Yang, P.-A., Hsu, H.-C., Kuo, H.-T., Girinath, P., and Fang, C.-J. (2012) Helix formation and capping energetics of arginine analogs with varying side chain length. *Amino Acids 43*, 195−206.
(8) Muñoz, V., and Serrano, L. (1994) Intrinsic secondary structure propensities of the amino acids, using statistical φ-ψ matrices: comparison with experimental scales. *Proteins 20*, 301−311.
(9) Kuo, L.-H., Li, J.-H., Kuo, H.-T., Hung, C.-Y., Tsai, H.-Y., Chiu, W.-C., Wu, C.-H., Wang, W.-R., Yang, P.-A., Yao, Y.-C., Wong, T. W., Huang, S.-J., Huang, S.-L., and Cheng, R. P. (2013) Effect of charged amino acid side chain length at non-hydrogen bonded strand positions on β-hairpin stability. *Biochemistry 52*, 7785−7797.
(10) Hardy, J., and Allsop, D. (1991) Amyloid deposition as the central event in the aetiology of Alzheimer's disease. *Trends Pharmacol. Sci. 12*, 383−388.
(11) Bartzokis, G., Lu, P. H., and Mintz, J. (2007) Human brain myelination and amyloid β deposition in Alzheimer's disease. *Alzheimers Dement. 3*, 122−125.
(12) Scherzinger, E., Lurz, R., Turmaine, M., Mangiarini, L., Hollenbach, B., Hasenbank, R., Bates, G. P., Davies, S. W., Lehrach, H., and Wanker, E. E. (1997) Huntingtin-encoded polyglutamine expansions form amyloid-like protein aggregates in vitro and in vivo. *Cell 90*, 549−558.
(13) Truant, R., Atwal, R. S., Desmond, C., Munsie, L., and Tran, T. (2008) Huntington's disease: Revisiting the aggregation hypothesis in polyglutamine neurodegenerative diseases. *FEBS J. 275*, 4252−4262.
(14) Irvine, G. B., El-Agnaf, O. M., Shankar, G. M., and Walsh, D. M. (2008) Protein aggregation in the brain: The molecular basis for Alzheimer's and Parkinson's diseases. *Mol. Med. 14*, 451−464.
(15) Mastaglia, F. L., Johnsen, R. D., Byrnes, M. L., and Kakulas, B. A. (2003) Prevalence of amyloid-β deposition in the cerebral cortex in Parkinson's disease. *Mov. Disord. 18*, 81−86.
(16) Hoppener, J. W., Ahren, B., and Lips, C. J. (2000) Islet amyloid and type 2 diabetes mellitus. *N. Engl. J. Med. 343*, 411−419.
(17) Haataja, L., Gurlo, T., Huang, C. J., and Butler, P. C. (2008) Islet amyloid in type 2 diabetes, and the toxic oligomer hypothesis. *Endocr. Rev. 29*, 303−316.
(18) Kitamoto, T., Tateishi, J., Tashima, T., Takeshita, I., Barry, R. A., DeArmond, S. J., and Prusiner, S. B. (1986) Amyloid plaques in Creutzfeldt-Jakob disease stain with prion protein antibodies. *Ann. Neurol. 20*, 204−208.
(19) Namba, Y., Tomonaga, M., Kawasaki, H., Otomo, E., and Ikeda, K. (1991) Apolipoprotein E immunoreactivity in cerebral amyloid deposits and neurofibrillary tangles in Alzheimer's disease and kuru plaque amyloid in Creutzfeldt-Jakob disease. *Brain Res. 541*, 163−166.
(20) Kim, C. A., and Berg, J. M. (1993) Thermodynamic β-sheet propensities measured using a zinc-finger host peptide. *Nature 362*, 267−270.
(21) Minor, D. L., and Kim, P. S. (1994) Measurement of the β-sheet-forming propensities of amino acids. *Nature 367*, 660−663.
(22) Smith, C. K., Withka, J. M., and Regan, L. (1994) A thermodynamic scale for the β-sheet forming tendencies of the amino acids. *Biochemistry 33*, 5510−5517.
(23) Clark, P. L., Liu, Z. P., Rizo, J., and Gierasch, L. M. (1997) Cavity formation before stable hydrogen bonding in the folding of a β-clam protein. *Nat. Struct. Biol. 4*, 883−886.
(24) Otzen, D. E., and Fersht, A. R. (1995) Side-chain determinants of β-sheet stability. *Biochemistry 34*, 5718−5724.
(25) Blasie, C. A., and Berg, J. M. (1997) Electrostatic interactions across a β-sheet. *Biochemistry 36*, 6218−6222.
(26) Smith, C. K., and Regan, L. (1995) Guidelines for protein design: The energetics of β sheet side chain interactions. *Science 270*, 980−982.
(27) Ramirez-Alvarado, M., Blanco, F. J., and Serrano, L. (1996) De novo design and structural analysis of a model β-hairpin peptide system. *Nat. Struct. Biol. 3*, 604−612.
(28) de Alba, E., Rico, M., and Jimenez, M. A. (1997) Cross-strand side-chain interactions versus turn conformation in β-hairpins. *Protein Sci. 6*, 2548−2560.
(29) Griffiths-Jones, S. R., Maynard, A. J., and Searle, M. S. (1999) Dissecting the stability of a β-hairpin peptide that folds in water: NMR and molecular dynamics analysis of the β-turn and β-strand contributions to folding. *J. Mol. Biol. 292*, 1051−1069.
(30) Gellman, S. H. (1998) Minimal model systems for β sheet secondary structure in proteins. *Curr. Opin. Chem. Biol. 2*, 717−725.
(31) Syud, F. A., Stanger, H. E., and Gellman, S. H. (2001) Interstrand side chain-side chain interactions in a designed β-hairpin: Significance of both lateral and diagonal pairings. *J. Am. Chem. Soc. 123*, 8667−8677.
(32) Cochran, A. G., Tong, R. T., Starovasnik, M. A., Park, E. J., McDowell, R. S., Theaker, J. E., and Skelton, N. J. (2001) A minimal peptide scaffold for β-turn display: Optimizing a strand position in disulfide-cyclized β-hairpins. *J. Am. Chem. Soc. 123*, 625−632.
(33) Cochran, A. G., Skelton, N. J., and Starovasnik, M. A. (2001) Tryptophan zippers: Stable, monomeric β-hairpins. *Proc. Natl. Acad. Sci. U. S. A. 98*, 5578−5583.
(34) Tatko, C. D., and Waters, M. L. (2002) Selective aromatic interactions in β-hairpin peptides. *J. Am. Chem. Soc. 124*, 9372−9373.
(35) Wouters, M. A., and Curmi, P. M. G. (1995) An analysis of side chain interactions and pair correlations within antiparallel β-sheets: The differences between backbone hydrogen-bonded and non-hydrogen-bonded residue pairs. *Proteins 22*, 119−131.
(36) Cootes, A. P., Curmi, P. M. G., Cunningham, R., Donnelly, C., and Torda, A. E. (1998) The dependence of amino acid pair correlations on structural environment. *Proteins 32*, 175−189.
(37) Hutchinson, E. G., Sessions, R. B., Thornton, J. M., and Woolfson, D. N. (1998) Determinants of strand register in antiparallel β-sheets of proteins. *Protein Sci. 7*, 2287−2300.
(38) Tatko, C. D., and Waters, M. L. (2003) The geometry and efficacy of cation-π interactions in a diagonal position of a designed β-hairpin. *Protein Sci. 12*, 2443−2452.
(39) Hughes, R. M., Benshoff, M. L., and Waters, M. L. (2007) Effects of chain length and N-methylation on a cation-π interaction in a β-hairpin peptide. *Chem.—Eur. J. 13*, 5753−5764.
(40) Searle, M. S., Griffiths-Jones, S. R., and Skinner-Smith, H. (1999) Energetics of weak interactions in a β-hairpin peptide: Electrostatic and hydrophobic contributions to stability from lysine salt bridges. *J. Am. Chem. Soc. 121*, 11615−11620.
(41) Tatko, C. D., and Waters, M. L. (2004) Comparison of C-H···π and hydrophobic interactions in a β-hairpin peptide: Impact on stability and specificity. *J. Am. Chem. Soc. 126*, 2028−2034.
(42) de Alba, E., Blanco, F. J., Jimenez, M. A., Rico, M., and Nieto, J. L. (1995) Interactions responsible for the pH dependence of the β-hairpin conformational population formed by a designed linear peptide. *Eur. J. Biochem. 233*, 283−292.
(43) Kiehna, S. E., and Waters, M. L. (2003) Sequence dependence of β-hairpin structure: Comparison of a salt bridge and an aromatic interaction. *Protein Sci. 12*, 2657−2667.

(44) Ramirez-Alvarado, M., Blanco, F. J., and Serrano, L. (2001) Elongation of the BH8 β-hairpin peptide: Electrostatic interactions in β-hairpin formation and stability. *Protein Sci. 10*, 1381−1392.
(45) Paliwal, S., Geib, S., and Wilcox, C. S. (1994) Molecular torsion balance for weak molecular recognition forces. Effects of "Tilted-T" edge-to-face aromatic interactions on conformational selection and solid-state structure. *J. Am. Chem. Soc. 116*, 4497−4498.
(46) Kim, E., Paliwal, S., and Wilcox, C. S. (1998) Measurements of molecular electrostatic field effects in edge-to-face aromatic interactions and CH-π interactions with implications for protein folding and molecular recognition. *J. Am. Chem. Soc. 120*, 11192−11193.
(47) Laughrey, Z. R., Kiehna, S. E., Riemen, A. J., and Waters, M. L. (2008) Carbohydrate-π Interactions: What are they worth? *J. Am. Chem. Soc. 130*, 14625−14633.
(48) Dill, K. A. (1990) Dominant forces in protein folding. *Biochemistry 29*, 7133−7155.
(49) Makhatadze, G. I., and Privalov, P. L. (1995) Energetics of protein structure. *Adv. Protein Chem. 47*, 307−425.
(50) Barlow, D. J., and Thornton, J. M. (1983) Ion-pairs in proteins. *J. Mol. Biol. 168*, 867−885.
(51) Marqusee, S., and Baldwin, R. L. (1987) Helix stabilization by Glu-···Lys+ salt bridges in short peptides of de novo design. *Proc. Natl. Acad. Sci. U. S. A. 84*, 8898−8902.
(52) Anderson, D. E., Becktel, W. J., and Dahlquist, F. W. (1990) pH-Induced denaturation of proteins: A single salt bridge contributes 3−5 kcal/mol to the free energy of folding of T4 lysozyme. *Biochemistry 29*, 2403−2408.
(53) Tissot, A. C., Vuilleumier, S., and Fersht, A. R. (1996) Importance of two buried salt bridges in the stability and folding pathway of barnase. *Biochemistry 35*, 6786−6794.
(54) Milla, M. E., Brown, B. M., and Sauer, R. T. (1994) Protein stability effects of a complete set of alanine substitutions in Arc repressor. *Nat. Struct. Biol. 1*, 518−523.
(55) Merkel, J. S., Sturtevant, J. M., and Regan, L. (1999) Sidechain interactions in parallel β sheets: The energetics of cross-strand pairings. *Structure 7*, 1333−1343.
(56) Russell, S. J., and Cochran, A. G. (2000) Designing stable β-hairpins: Energetic contributions from cross-strand residues. *J. Am. Chem. Soc. 122*, 12600−12601.
(57) Ciani, B., Jourdan, M., and Searle, M. S. (2003) Stabilization of β-hairpin peptides by salt bridges: Role of preorganization in the energetic contribution of weak interactions. *J. Am. Chem. Soc. 125*, 9038−9047.
(58) Searle, M. S., Griffiths-Jones, S. R., and Skinner-Smith, H. (1999) Energetics of weak interactions in a β-hairpin peptide: Electrostatic and hydrophobic contributions to stability from lysine salt bridges. *J. Am. Chem. Soc. 121*, 11615−11620.
(59) Chakrabartty, A., Kortemme, T., and Baldwin, R. L. (1994) Helix propensities of the amino acids measured in alanine-based peptides without helix-stabilizing side-chain interactions. *Protein Sci. 3*, 843−852.
(60) Doig, A. J., and Baldwin, R. L. (1995) N- and C-capping preferences for all 20 amino acids in α-helical peptides. *Protein Sci. 4*, 1325−1336.
(61) Sueki, M., Lee, S., Powers, S. P., Denton, J. B., Konishi, Y., and Scheraga, H. A. (1984) Helix coil stability constants for the naturally occurring amino acids in water 22. Histidine parameters from random poly[(hydroxybutyl)glutamine-*co*-L-histidine]. *Macromolecules 17*, 148−155.
(62) Padmanabhan, S., York, E. J., Stewart, J. M., and Baldwin, R. L. (1996) Helix propensities of basic amino acids increase with the length of the side-chain. *J. Mol. Biol. 257*, 726−734.
(63) Cheng, R. P., Girinath, P., and Ahmad, R. (2007) Effect of lysine side chain length on intra-helical glutamate-lysine ion pairing interactions. *Biochemistry 46*, 10528−10537.
(64) Atherton, E., Fox, H., Harkiss, D., Logan, C. J., Sheppard, R. C., and Williams, B. J. (1978) A mild procedure for solid phase peptide synthesis: Use of fluorenylmethoxycarbonylamino-acids. *J. Chem. Soc., Chem. Commun.*, 537−539.
(65) Fields, G. B., and Noble, R. L. (1990) Solid phase peptide synthesis utilizing 9-fluorenylmethoxycarbonyl amino acids. *Int. J. Pept. Protein Res. 35*, 161−214.
(66) Volkmer-Engert, R., Landgraf, C., and Schneider-Mergener, J. (1998) Charcoal surface-assisted catalysis of intramolecular disulfide bond formation in peptides. *J. Pept. Res. 51*, 365−369.
(67) Aue, W. P., Bartholdi, E., and Ernst, R. R. (1976) Two-dimensional spectroscopy. Application to nuclear magnetic resonance. *J. Chem. Phys. 64*, 2229−2246.
(68) Bax, A., and Davis, D. G. (1985) MLEV-17-based two-dimensional homonuclear magnetization transfer spectroscopy. *J. Magn. Reson. 65*, 355−360.
(69) Jeener, J., Meier, B. H., Bachmann, P., and Ernst, R. R. (1979) Investigation of exchange processes by two-dimensional NMR spectroscopy. *J. Chem. Phys. 71*, 4546−4553.
(70) Bothner-By, A. A., Stephens, R. L., Lee, J. M., Warren, C. D., and Jeanloz, R. W. (1984) Structure determination of a tetrasaccharide: Transient nuclear overhauser effects in the rotating frame. *J. Am. Chem. Soc. 106*, 811−813.
(71) Piotto, M., Saudek, V., and Sklenar, V. (1992) Gradient-tailored excitation for single-quantum NMR spectroscopy of aqueous-solutions. *J. Biomol. NMR 2*, 661−665.
(72) Sklenar, V., Piotto, M., Leppik, R., and Saudek, V. (1993) Gradient-tailored water suppression for $^{1}H-^{15}N$ HSQC experiments optimized to retain full sensitivity. *J. Magn. Reson. Ser. A 102*, 241−245.
(73) Dalgarno, D. C., Levine, B. A., and Williams, R. J. (1983) Structural information from NMR secondary chemical shifts of peptide α C-H protons in proteins. *Biosci. Rep. 3*, 443−452.
(74) Wishart, D. S., Sykes, B. D., and Richards, F. M. (1991) Relationship between nuclear magnetic resonance chemical shift and protein secondary structure. *J. Mol. Biol. 222*, 311−333.
(75) Ramirez-Alvarado, M., Kortemme, T., Blanco, F. J., and Serrano, L. (1999) β-Hairpin and β-sheet formation in designed linear peptides. *Bioorg. Med. Chem. 7*, 93−103.
(76) Syud, F. A., Espinosa, J. F., and Gellman, S. H. (1999) NMR-based quantification of β-sheet populations in aqueous solution through use of reference peptides for the folded and unfolded states. *J. Am. Chem. Soc. 121*, 11577−11578.
(77) Kim, Y. M., and Prestegard, J. H. (1989) Measurement of vicinal couplings from cross peaks in COSY spectra. *J. Magn. Reson. 84*, 9−13.
(78) Horovitz, A. (1996) Double-mutant cycles: A powerful tool for analyzing protein structure and function. *Fold Des. 1*, R121−R126.
(79) Cockroft, S. L., and Hunter, C. A. (2007) Chemical double-mutant cycles: Dissecting non-covalent interactions. *Chem. Soc. Rev. 36*, 172−188.
(80) Hobohm, U., and Sander, C. (1994) Enlarged representative set of protein structures. *Protein Sci. 3*, 522−524.
(81) Griep, S., and Hobohm, U. (2010) PDBselect 1992−2009 and PDBfilter-select. *Nucleic Acids Res. 38*, D318−D319.
(82) Kabsch, W., and Sander, C. (1983) Dictionary of protein secondary structure: Pattern recognition of hydrogen-bonded and geometrical features. *Biopolymers 22*, 2577−2637.
(83) Joosten, R. P., Beek, T. A. H. T., Krieger, E., Hekkelman, M. L., Hooft, R. W. W., Schneider, R., Sander, C., and Vriend, G. (2011) A series of PDB related databases for everyday needs. *Nucleic Acids Res. 39*, D411−D419.
(84) Efron, B., and Gong, G. (1983) A leisurely look at the bootstrap, the jackknife, and cross-validation. *Am. Stat. 37*, 36−48.
(85) Klugh, H. E. (1970) Statistics-The essentials for research, in *Statistics-The Essentials for Research*, John Wiley & Sons, Inc, New York.
(86) Kuebler, R. R., and Smith, H. (1976) Statistics-A beginning, in *Statistics-A Beginning*, John Wiley & Sons, Inc, New York.
(87) Stanger, H. E., and Gellman, S. H. (1998) Rules for antiparallel β-sheet design: D-Pro-Gly is superior to L-Asn-Gly for β-hairpin nucleation. *J. Am. Chem. Soc. 120*, 4236−4237.

(88) Ciani, B., Jourdan, M., and Searle, M. S. (2003) Stabilization of β-hairpin peptides by salt bridges: Role of preorganization in the energetic contribution of weak interactions. *J. Am. Chem. Soc. 125*, 9038−9047.
(89) Rose, G. D., Gierasch, L. M., and Smith, J. A. (1985) Turns in peptides and proteins. *Adv. Protein Chem. 37*, 1−109.
(90) Russell, S. J., Blandl, T., Skelton, N. J., and Cochran, A. G. (2003) Stability of cyclic β-hairpins: Asymmetric contributions from side chains of a hydrogen-bonded cross-strand residue pair. *J. Am. Chem. Soc. 125*, 388−395.
(91) Wüthrich, K. (1986) *NMR of Proteins and Nucleic Acids*, John Wiley & Sons, New York.
(92) Yao, J., Dyson, H. J., and Wright, P. E. (1997) Chemical shift dispersion and secondary structure prediction in unfolded and partly folded proteins. *FEBS Lett. 419*, 285−289.
(93) Smith, J. S., and Scholtz, J. M. (1998) Energetics of polar side-chain interactions in helical peptides: Salt effects on ion pairs and hydrogen bonds. *Biochemistry 37*, 33−40.